Electronic Supplementary Material (ESI) for Materials Advances.

Supporting Information

Graphitic carbon nitride embedded-Ag nanoparticle decorated-$ZnWO_4$ nanocomposite based photoluminescence sensing of Hg^{2+}

Uday Kumar Ghorui[†], Jit Satra[†], Papri Mondal[†], Sourav Mardanya[†], Arpita Sarkar[†], Divesh N. Srivastava[‡], Bibhutosh Adhikary[†*] and Anup Mondal[†*]

[†]Department of Chemistry, Indian Institute of Engineering Science and Technology, Shibpur, Howrah-711103, West Bengal, India.

[‡]Department of Analytical Science, Central Salt, and Marine Chemicals Research Institute, Gijubhai, Badheka Marg, Bhavnagar 364002, Gujarat, India

Corresponding Authors

[*]Email: bibhutosh@chem.iiests.ac.in, bibhutoshadhikary@gmail.com Mob: +918902524532

[*]Email: anupmondal2000@yahoo.co.in, anup@chem.iiests.ac.in Mob: +919681420714

Materials: Zinc nitrate hexahydrate ($Zn(NO_3)_2.6H_2O$), sodium tungstate dihydrate ($Na_2WO_4.2H_2O$), liquid ammonia (NH_3), melamine powder, sulfuric acid (H_2SO_4), nitric acid (HNO_3), tri-sodium citrate, cobaltous chloride ($CoCl_2$), calcium chloride ($CaCl_2$), cadmium chloride ($CdCl_2$), cupric chloride ($CuCl_2$), ferric chloride ($FeCl_3$), manganous chloride ($MnCl_2$), potassium chloride (KCl), lead chloride ($PbCl_2$) and nickel(II) chloride ($NiCl_2$) were purchased from Merck Specialties Private Limited, India. All the chemicals were used as purchased and without further purification. Mili-Q water was used for all experiments unless mentioned otherwise. Silver nitrate ($AgNO_3$, 99%), mercuric chloride ($HgCl_2$), and sodium borohydride ($NaBH_4$) were purchased from Sigma–Aldrich.

Synthesis of g-C_3N_4/Ag/$ZnWO_4$ nanocomposite: $ZnWO_4$ nanorods were prepared by a simple hydrothermal method according to the earlier report.[1] In brief, 1mmol each of zinc nitrate hexahydrate ($Zn(NO_3)_2.6H_2O$) and sodium tungstate dihydrate ($Na_2WO_4.2H_2O$) were dissolved in 20 ml 1:4 ammonia-water solution in two separate beakers. Then, the clear Na_2WO_4 solution was added drop-wise to $Zn(NO_3)_2$ solution and stirred vigorously at room temperature for 30 min maintaining a pH of 10.0 by adding NH_4OH. The white slurry as obtained from the mixture of the solutions was transferred to 50 ml Teflon-lined autoclave and maintained at 180 ^{0}C for 12 h. The autoclave was then cooled to room temperature naturally and the as-prepared sample was separated by centrifugation and washed with Mili-Q water, followed by anhydrous ethanol. The white sample was then dried at 60 °C for 6 h.

To synthesize bulk g-C_3N_4, 7.5 g of melamine powder was kept into a porcelain boat with a cover and heated to 600 ^{0}C in a muffle furnace for 6 h with a heating rate of 3°C min^{-1}. The obtained yellow product was then ground to a fine powder for further processing and characterization.

To synthesize the g-C_3N_4/$ZnWO_4$ nanocomposite, the following procedure was carried out. At first, the as-prepared $ZnWO_4$ nanorods were dispersed in 20 ml Mili-Q water in an ultra sonicator bath for about1 h. In another beaker, x mg (x = 20, 40, 80 mg) g-C_3N_4 was mixed in 80 ml aqueous solution containing1 ml conc. H_2SO_4 and 3 ml conc. HNO_3 acid solutions, by sonication for 2 h. A white suspension was obtained after sonication. Then, the previously dispersed $ZnWO_4$ solution was added to the g-C_3N_4 suspension. The suspension mixture was then placed on a hot plate at ~90 ^{0}C for 12 h with continuous magnetic stirring to evaporate the

solution to dryness. Finally, the yellowish product obtained was washed with 1:1 ethanol-water solution to remove excess acid and collected by centrifugation and dried at 60 °C for 6 h. The samples were denoted as g-C_3N_4/$ZnWO_4$ -0.25, -0.50, -1 (the notation as per g-C_3N_4 concentration in mg/ml).

Ag nanoparticles were prepared with sodium borohydride ($NaBH_4$) as a reducing agent and sodium citrate as a stabilizer.[2] Briefly, 0.5 ml 0.01 (M) aqueous $AgNO_3$ solution was mixed with 20 ml 1 mM tri-sodium citrate with magnetic stirring. After 20 minutes, 0.5 ml 0.01 (M) $NaBH_4$ solution was added to this solution under vigorous magnetic stirring at ambient temperature, resulting in a dark yellow-colored solution, indicating the formation of spherical Ag NPs. All the experiments were performed in a clean atmosphere to avoid contamination which may interfere with the toxicity of the nanoparticles.

As prepared $ZnWO_4$ NPs were first dispersed in 40 ml water and the suspension was stirred for 30 minutes at 60 ^{0}C in an inert atmosphere. To this suspension, the freshly prepared Ag NPs were injected. After 15 minutes, the final mixture was heated at 90 ^{0}C for 30 minutes. The grayish Ag/$ZnWO_4$ nanocomposite was collected by centrifugation and washed with water and dried at 60 ^{0}C for 4 h.

To prepare g-C_3N_4/Ag/$ZnWO_4$ nanocomposite, first, g-C_3N_4 was sonicated for 2 h in a beaker to disperse in 40 ml water containing concentrated 1 ml H_2SO_4 and 3 ml HNO_3. Another solution of Ag/$ZnWO_4$ was prepared by ultra-sonication in 20 ml water. To the previous solution of g-C_3N_4, the second solution was added and stirred till evaporated to dryness, keeping a constant temperature of 90°C. A pale yellowish crude product appeared. To obtain the pure desired product the excess g-C_3N_4 and the surfactant were eliminated by annealing at 300 °C for 1 h in an N_2 atmosphere.

Sample Characterization: The phases and crystallinity of the synthesized nanomaterials were determined by X-ray diffraction. X-ray scans of the samples were recorded from 5˚ to 60˚ 2θ by a Philips PW 1140 parallel beam X-ray diffractometer with monochromatic CuKα radiation (λ=1.540598 Å) at room temperature. To observe the surface morphology of the materials, high-resolution transmission electron microscopy (HRTEM) was performed at 200 kV by a TEM-JEOL JEM-2100. Field emission scanning electron microscopy (FESEM) and elemental

compositions by energy dispersive spectrometry (EDS) was carried out using a 20 kV FE-SEM, JEOL JSM 7100F. X-ray photoelectron spectroscopy (XPS) was executed with a Perkin-Elmer Physical Electronics 5600 spectrometer to confirm the existence of Ag(0) in the composite. The ASAP 2010 surface area (BET isotherm) analyzer was used to examine the N_2 adsorption/desorption characteristics. JASCO V-630 UV-Vis spectrophotometer was used to investigate absorption spectra at room temperature of the materials and the photoluminescence (PL) applications and lifetime measurements were carried out with a Horiba Fluorolog instrument.

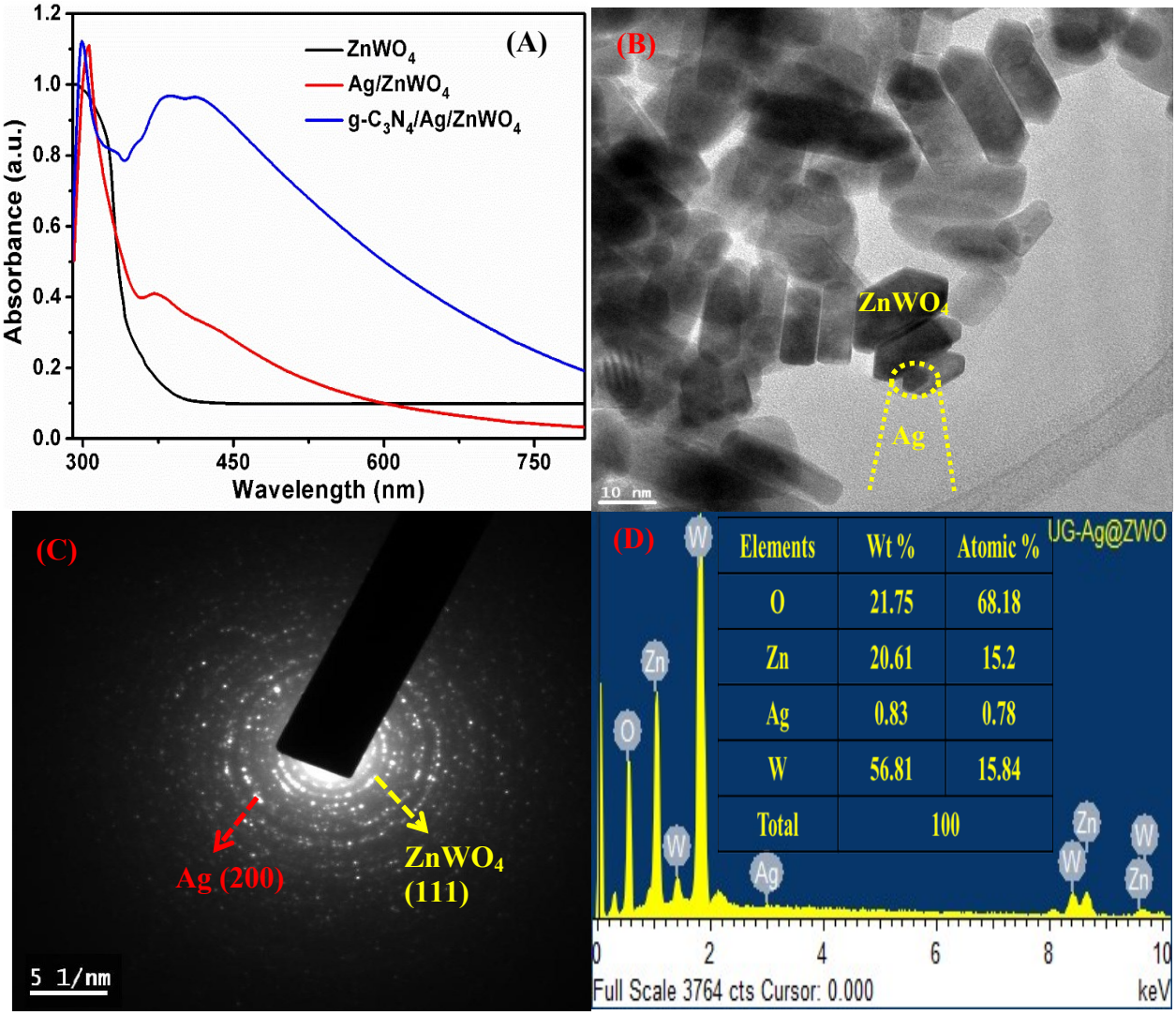

Figure S1: UV-Vis spectroscopy of pure $ZnWO_4$, $Ag/ZnWO_4$ and $g\text{-}C_3N_4/Ag/ZnWO_4$ (A); TEM image (B), SAED pattern (C), and EDX (D) of $Ag/ZnWO_4$.

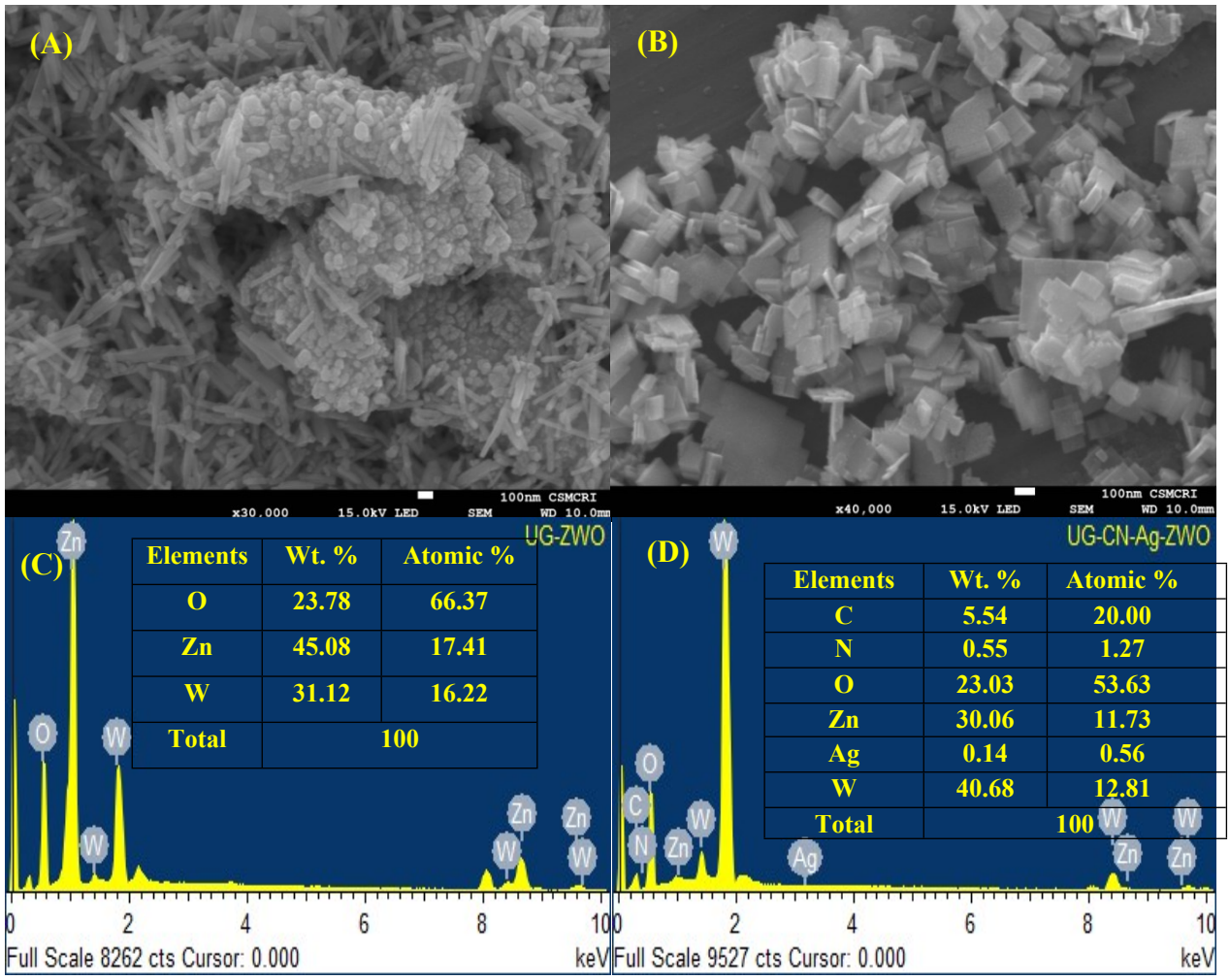

Figure S2: (A) FESEM and (C) EDS results of $ZnWO_4$ nanorods and (B) FESEM and (D) EDS results of g-C_3N_4/Ag/$ZnWO_4$ square nanoplates.

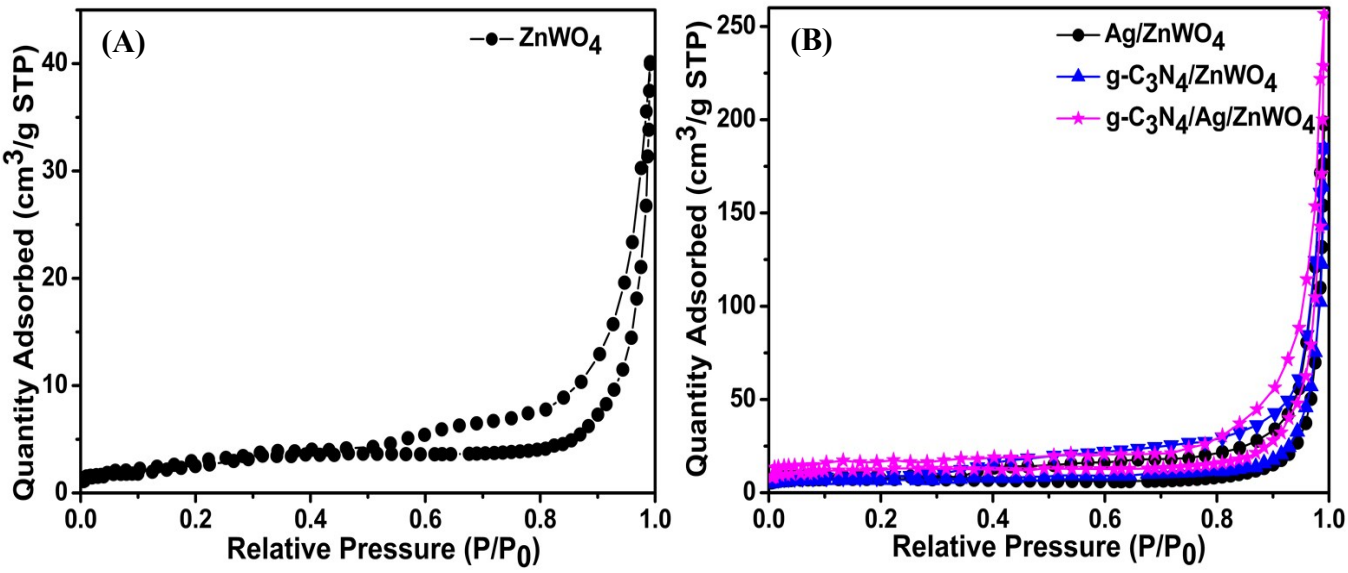

Figure S3: (A) BET-isotherms of $ZnWO_4$ and (B) Ag and g-C_3N_4 composited $ZnWO_4$, respectively.

Table S1: Comparison of the BET surface areas with ICP data of pure and hybrid $ZnWO_4$ nanomaterials

Materials	Weight % of Ag	Atomic Ratio of Ag/Zn	Surface Area (m^2/g)
$ZnWO_4$	——	——	29.2
$Ag/ZnWO_4$	2.86	0.051	39.1
g-$C_3N_4/ZnWO_4$	——	——	43.8
g-C_3N_4/Ag/$ZnWO_4$	2.71	0.047	55.7

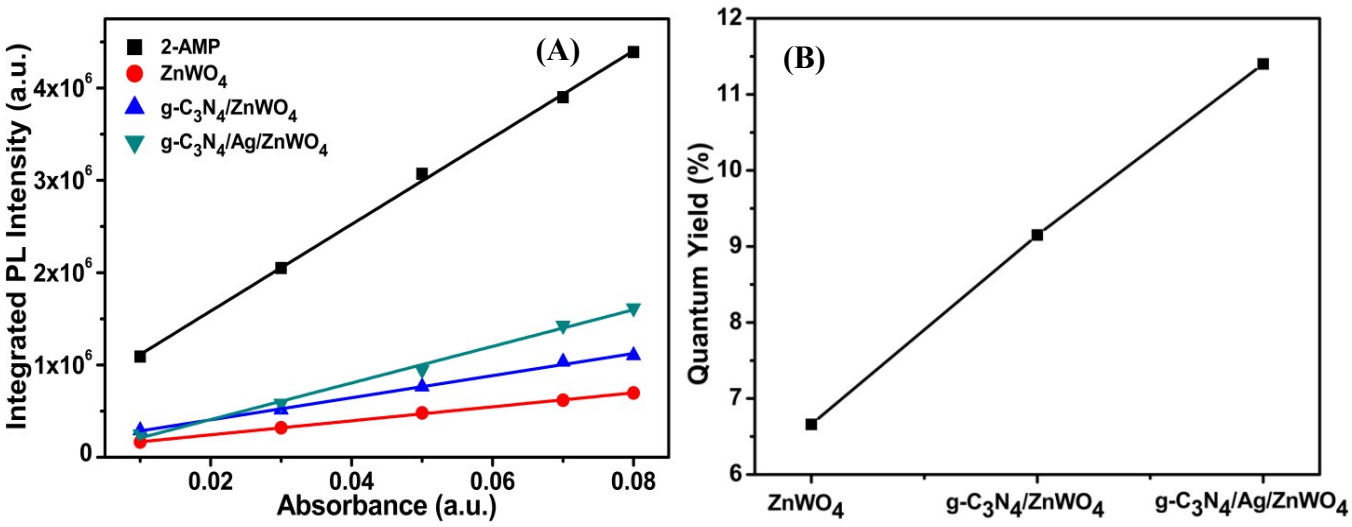

Figure S4: (A) Plots of PL Quantum Yields of various $ZnWO_4$ nanocomposites, (B) Plot of Quantum Yield percentage versus loading of g-C_3N_4 and Ag NPs.

Table S2: Quantum yield comparison table for the various $ZnWO_4$ nanocomposites.

Samples	Gradient	Φ_x (%)	R^2
2-AMP	46980000		0.9986
$ZnWO_4$	7580540	6.6	0.9991
g-C_3N_4/$ZnWO_4$	10407870	9.1	0.9933
g-C_3N_4/Ag/$ZnWO_4$	12875340	11.4	0.9878

Table S3: Radiative Fluorescence Lifetime and Relative Percentage of Photoinduced Charge Carriers in pure $ZnWO_4$ and the various composited $ZnWO_4$.

Fluorescence NPs	χ^2	α_1	τ_1(ns)	α_2	τ_2(ns)	α_3	τ_3(ns)	<τ> (ns)
$ZnWO_4$	1.09	28.30	2.35	15.04	9.60	56.66	0.52	**6.5**
g-C_3N_4/$ZnWO_4$	1.06	32.69	3.28	22.85	9.50	44.46	0.55	**7.3**
Ag/$ZnWO_4$	1.02	38.14	3.90	22.70	11.25	39.16	0.84	**8.1**
g-C_3N_4/Ag/$ZnWO_4$	1.06	54.92	5.72	24.50	15.42	20.58	1.25	**10.7**

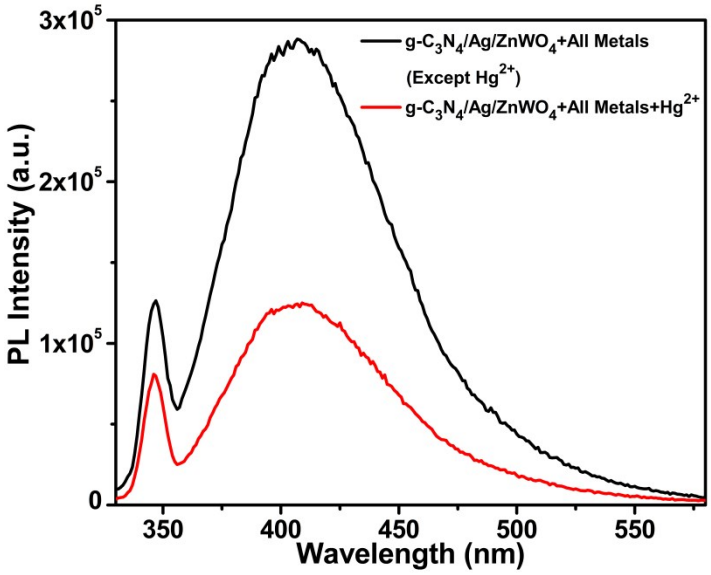

Figure S5: PL emission of g-C_3N_4/Ag/$ZnWO_4$ in presence of Hg^{2+} and other metal ions (λ_{ex}=360 nm, [M^{n+}]=1mM) M^{n+} = Ca^{2+}, Cd^{2+}, Fe^{2+}, Co^{2+}, Cu^{2+}, K^{+}, Mn^{2+}, Ni^{2+}, Pb^{2+} and Hg^{2+}.

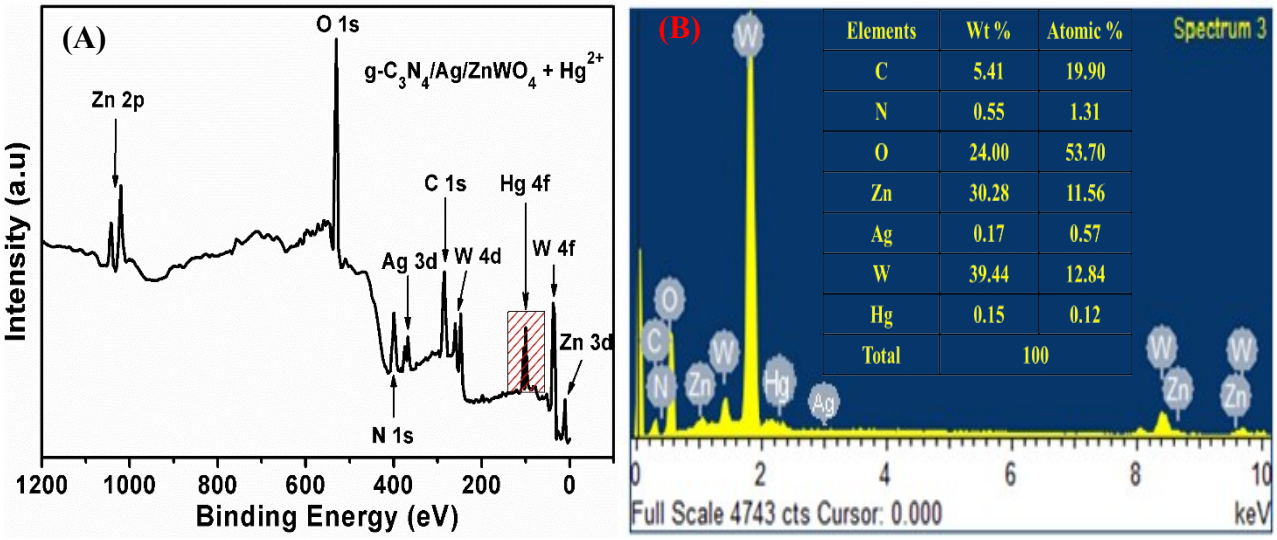

Figure S6: XPS analysis of g-C_3N_4/Ag/$ZnWO_4$ after adding Hg(II) salt in presence of other metal ions (A) overall scan; (B) EDX (inset EDX result) of g-C_3N_4/Ag/$ZnWO_4$ in presence of Hg(II) salt.

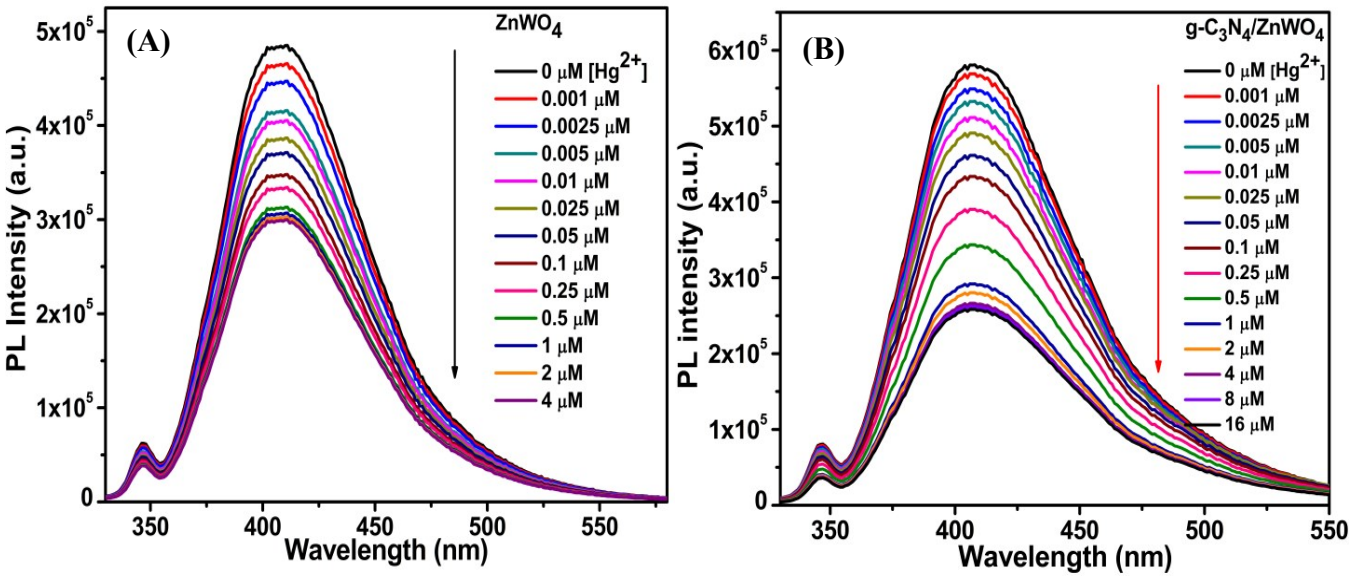

Figure S7: Quantitative detection of Hg^{2+} by photoluminescence in buffer (pH = 7.2) solutions containing (A) $ZnWO_4$ and (B) g-C_3N_4/ $ZnWO_4$.

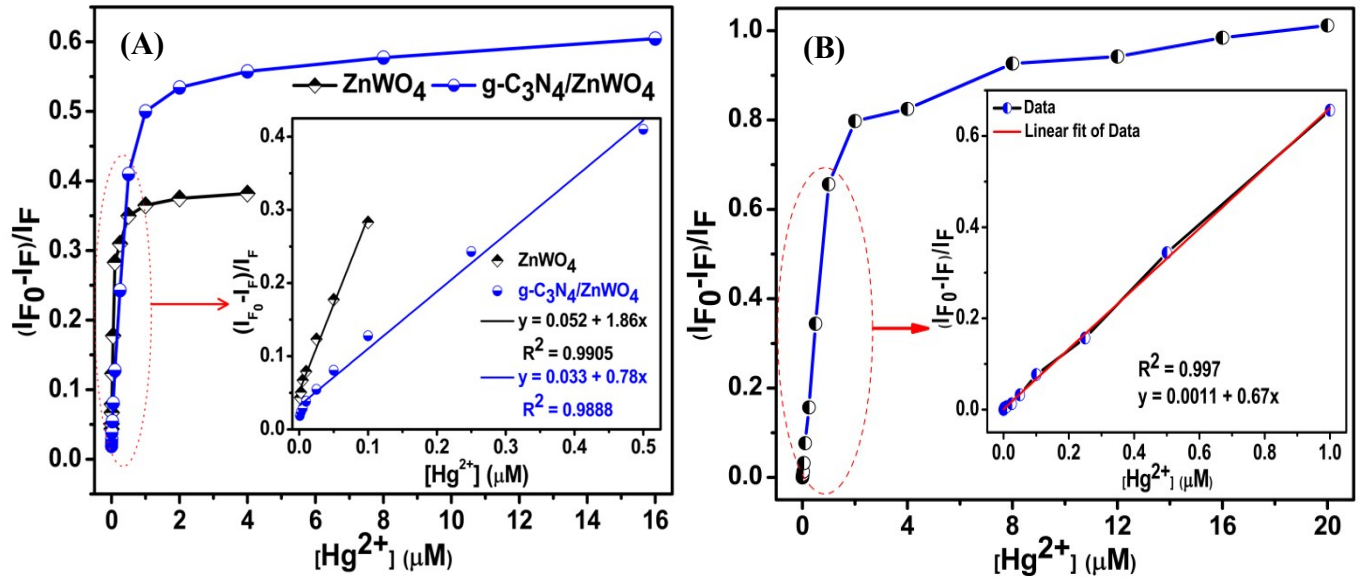

Figure S8: (A) Calibration curves of $ZnWO_4$ (black curve) and g-C_3N_4/$ZnWO_4$ (blue curve) for the detection of Hg^{2+} (inset contains linear plots of relative intensity vs. conc. of Hg^{2+}). (B) Calibration curve of g-C_3N_4/Ag/$ZnWO_4$ for Hg^{2+} sensing in tap water.

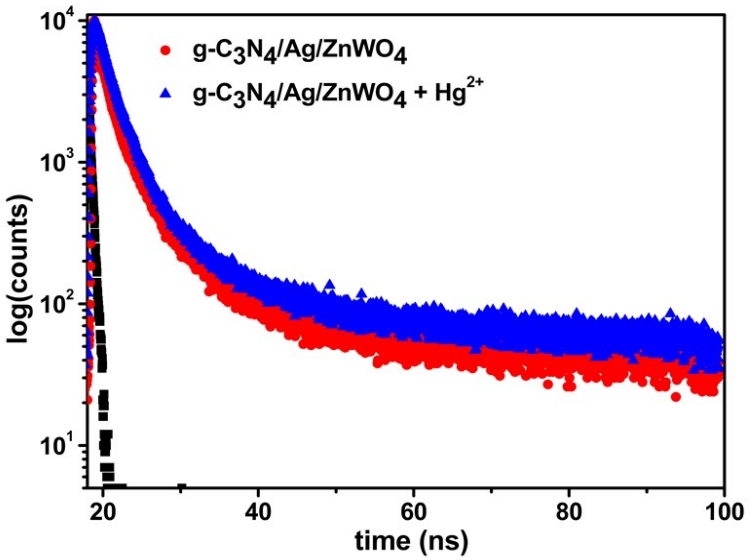

Figure S9: Lifetime measurement of g-C_3N_4/Ag/$ZnWO_4$ nanocomposite before and after PL quenching.

Table S4: Summary of triple exponential fitting of time-resolved fluorescence of g-C_3N_4/Ag/$ZnWO_4$ without and with the presence of Hg^{2+}.

Fluorescence NPs	χ^2	α_1	τ_1(ns)	α_2	τ_2(ns)	α_3	τ_3(ns)	$\langle\tau\rangle$ (ns)
g-C_3N_4/Ag/$ZnWO_4$	1.06	54.92	5.72	24.50	15.42	20.58	1.25	**10.7**
g-C_3N_4/Ag/$ZnWO_4$ + Hg^{2+}	1.0007	52.43	6.10	24.46	16.08	23.11	0.82	**11.3**

From Figure S6, it is well justified that an increase in the lifetime of the carriers of g-C_3N_4/Ag/$ZnWO_4$ takes place after the addition of Hg^{2+} ions. The average lifetime of the carriers was calculated using equation (1). From Table S4 it is clear that the fluorescence lifetime is fitted with three exponentials. The three different decay lifetimes of g-C_3N_4/Ag/$ZnWO_4$ are τ_1 = **5.72 ns,** τ_2 = **15.42 ns,** and τ_3 = **1.25ns**, respectively with an average fluorescence lifetime $\langle\tau\rangle$ = **10.7 ns**. On addition of 10 μM Hg^{2+}, a triple exponential decay was observed with lifetimes of τ_1 = **6.10 ns,** τ_2 = **16.08 ns** and τ_3 = **0.82 ns**, respectively with an average lifetime $\langle\tau\rangle$ = **11.3 ns**. Thus the average time-resolved fluorescence of g-C_3N_4/Ag/$ZnWO_4$ increased by about **0.6 ns** after quenching of PL emission. The enhanced decay lifetime of g-C_3N_4/Ag/$ZnWO_4$ on the

addition of Hg^{2+} can be attributed to the presence of the heavy metal ion effect. This increase in a lifetime can be explained based on a better intersystem crossing from the excited singlet state to the triplet state. Based on the static quenching mechanism, these observations are indicative of ground-state complex formation between Hg^{2+} and g-C_3N_4/Ag/$ZnWO_4$; therefore, no decrease in fluorescence lifetime would be observed, as expected for a dynamic quenching process.[3] On addition of Hg^{2+} to the g-C_3N_4/Ag/$ZnWO_4$ nanocomposite the time-resolved fluorescence of each of the component, as well as the average lifetime also increased, which can be explained based on metallophilic effect with Ag by the formation of Ag-Hg nanoalloy[4] (as expected from our case in XPS analysis figure 8A). Therefore, it can be concluded that the increased average lifetime indicates a more populated upper excited state of the second component during the grafting of Hg^{2+} with the nanocomposite.

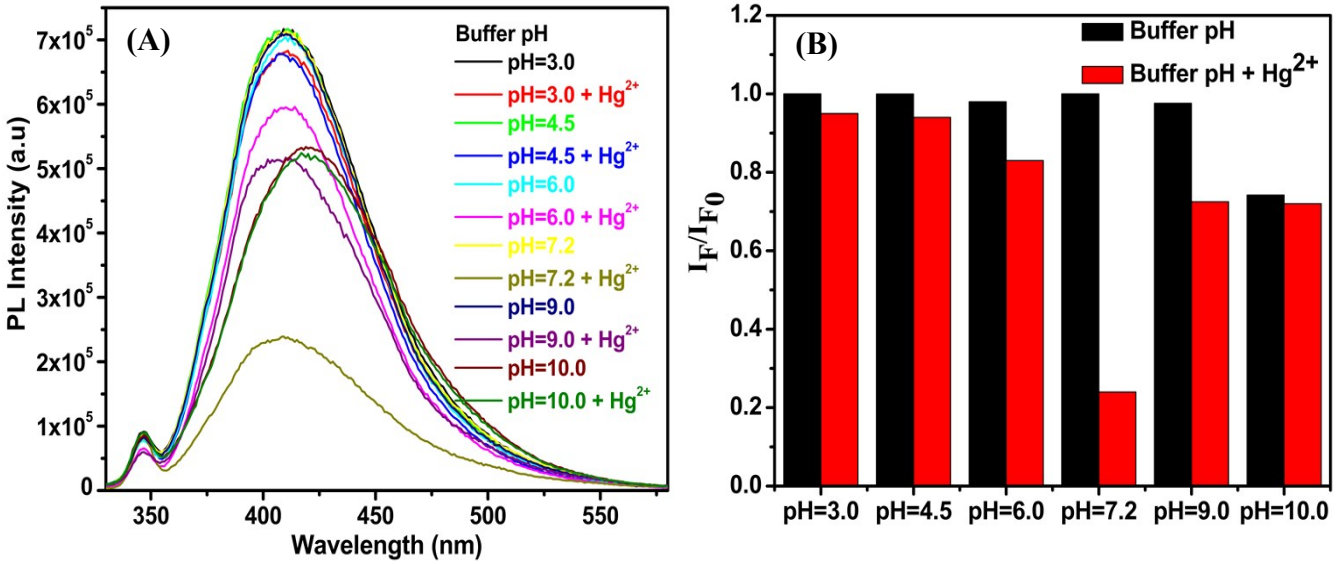

Figure S10: (A) PL emission spectra of g-C_3N_4/Ag/$ZnWO_4$ in different buffer pH and presence of Hg^{2+} at the respective pH, (B) Corresponding histograms of respective PL spectra.

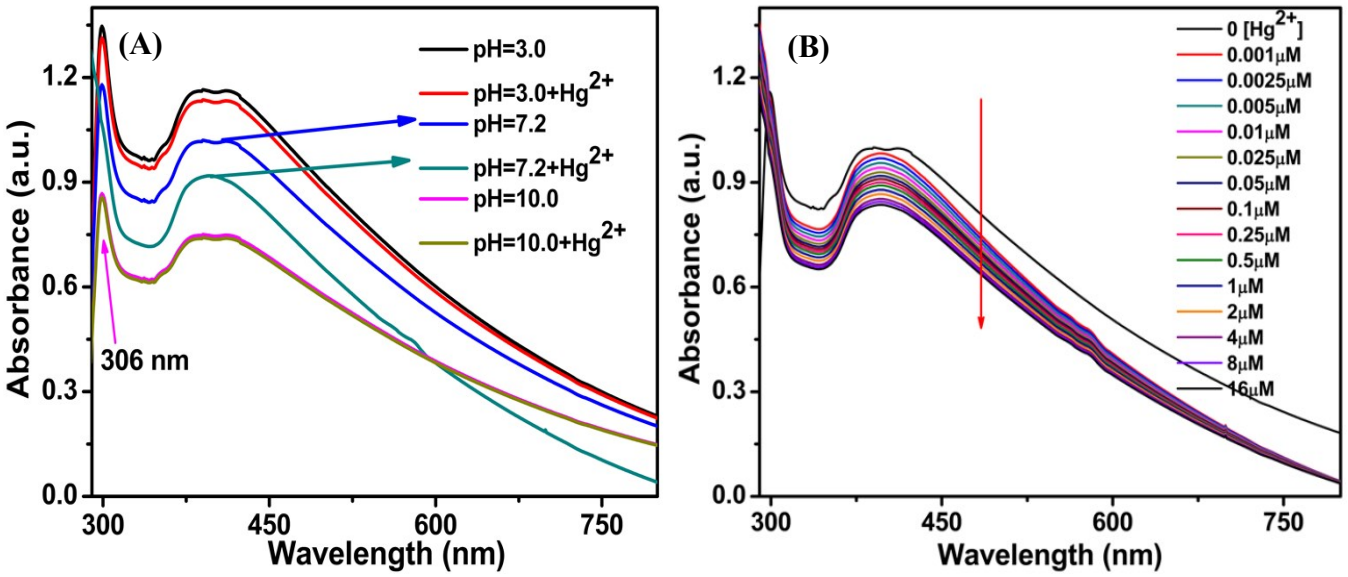

Figure S11: (A) UV-visible spectra of suspended g-C_3N_4/Ag/$ZnWO_4$ in solution at different pH values, pH-3.0, pH-7.2, pH-10.0, and corresponding spectra after addition of 20 μL of 10 μM Hg^{2+}. (B) UV-visible spectra of g-C_3N_4/Ag/$ZnWO_4$ in presence of different concentrations of Hg^{2+} ions.

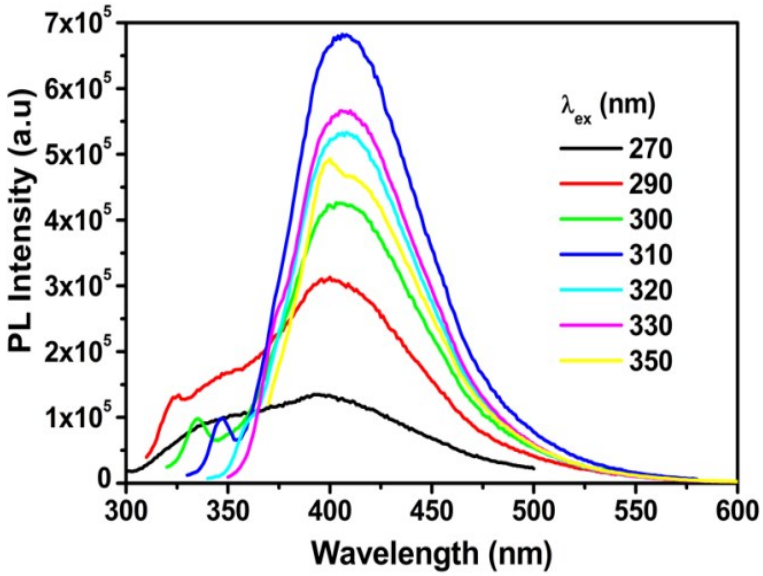

Figure S12: PL emission spectra of g-C_3N_4/Ag/$ZnWO_4$ for different excitation wavelengths.

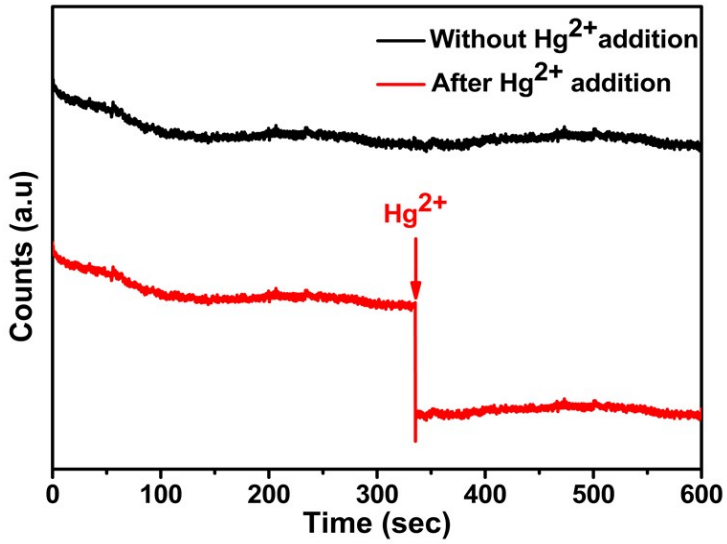

Figure S13: Time-resolved fluorescence stability test of g-C_3N_4/Ag/$ZnWO_4$ in the absence and presence of Hg^{2+}.

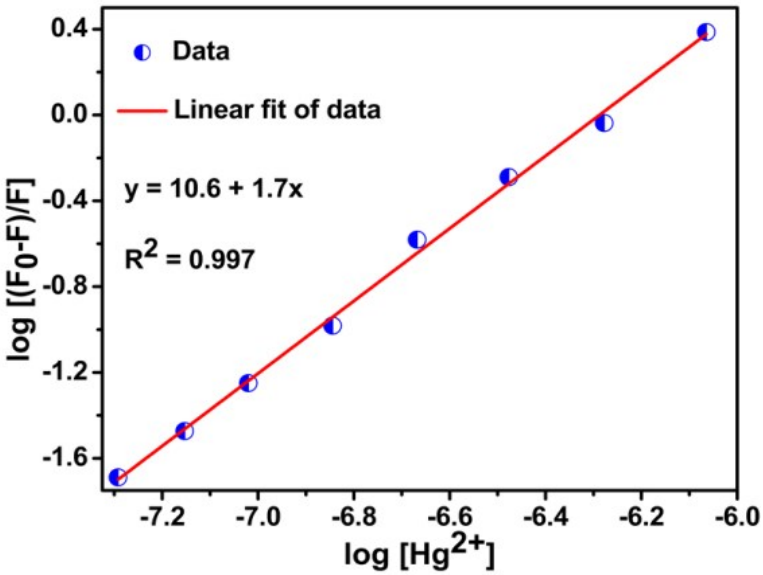

Figure S14: Binding constant and binding site calculation using PL data.

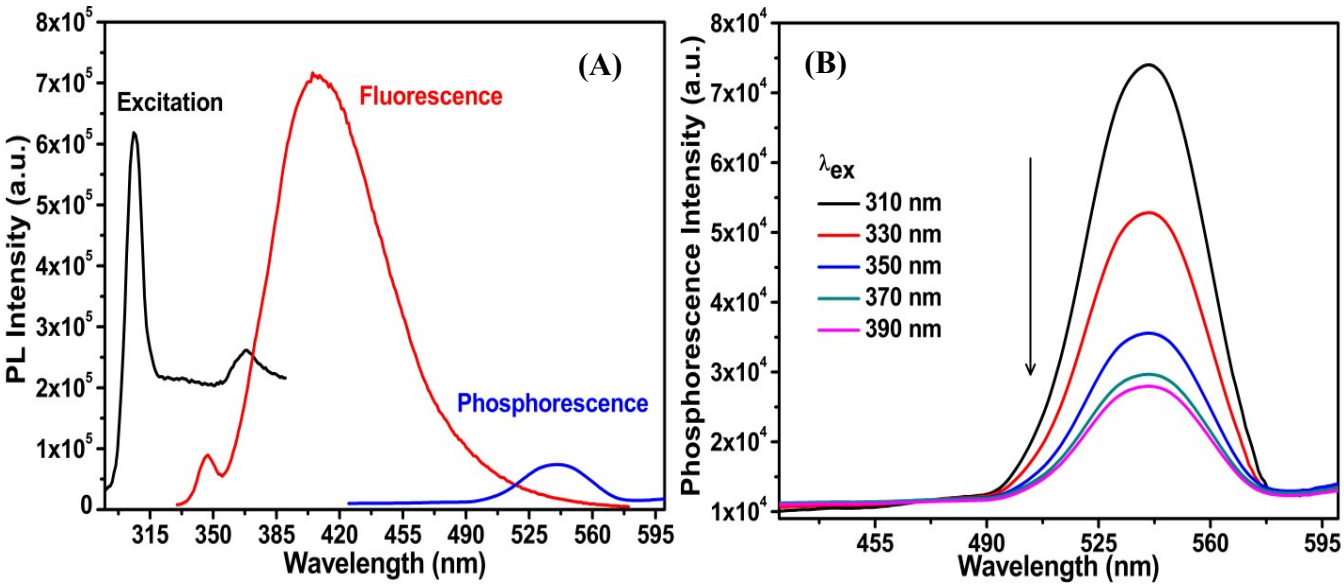

Figure S15: (A) PL excitation spectrum (black) and fluorescence emission (red) and phosphorescence (blue) emission spectra of g-C_3N_4/Ag/$ZnWO_4$ nanocomposite (λ_{ex} = 310 nm, λ_{emF} = 408 nm, λ_{emP} = 520 nm). (B) Change of phosphorescence intensity for different excitation wavelengths.

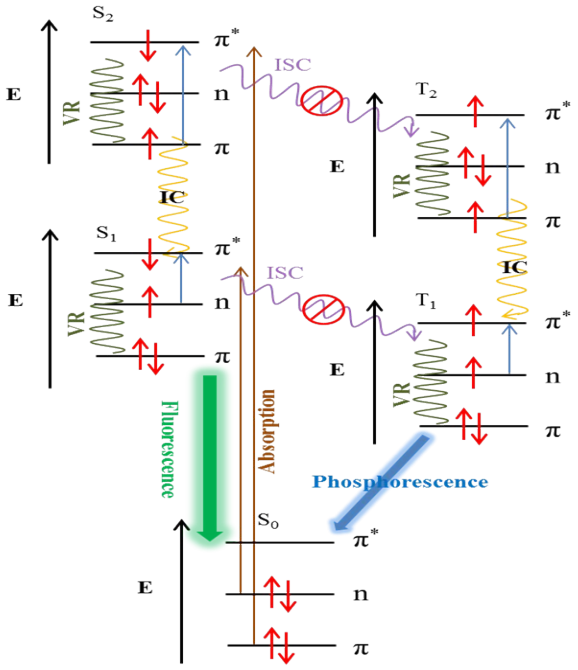

Scheme S1: Schematic representation of partial energy level diagram for PL in a molecular system for the explanation of Fluorescence and Room Temperature Phosphorescence (RTP) of g-C_3N_4/Ag/$ZnWO_4$.

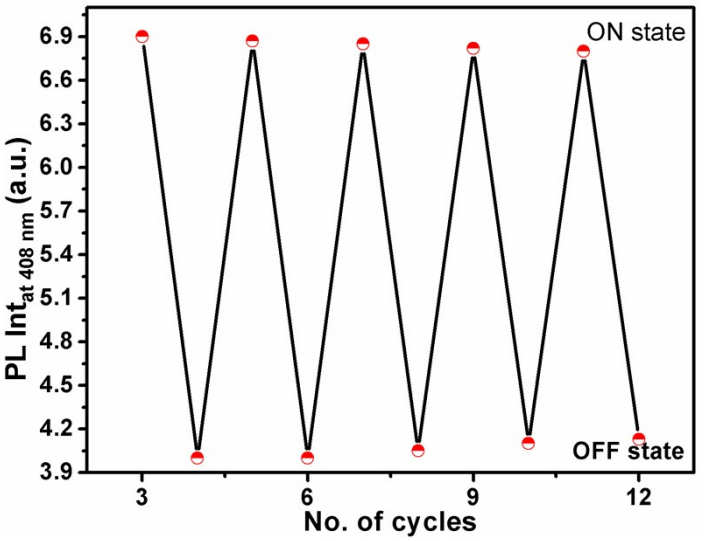

Figure S16: Recyclability test of g-C_3N_4/Ag/$ZnWO_4$ for the detection of Hg(II).

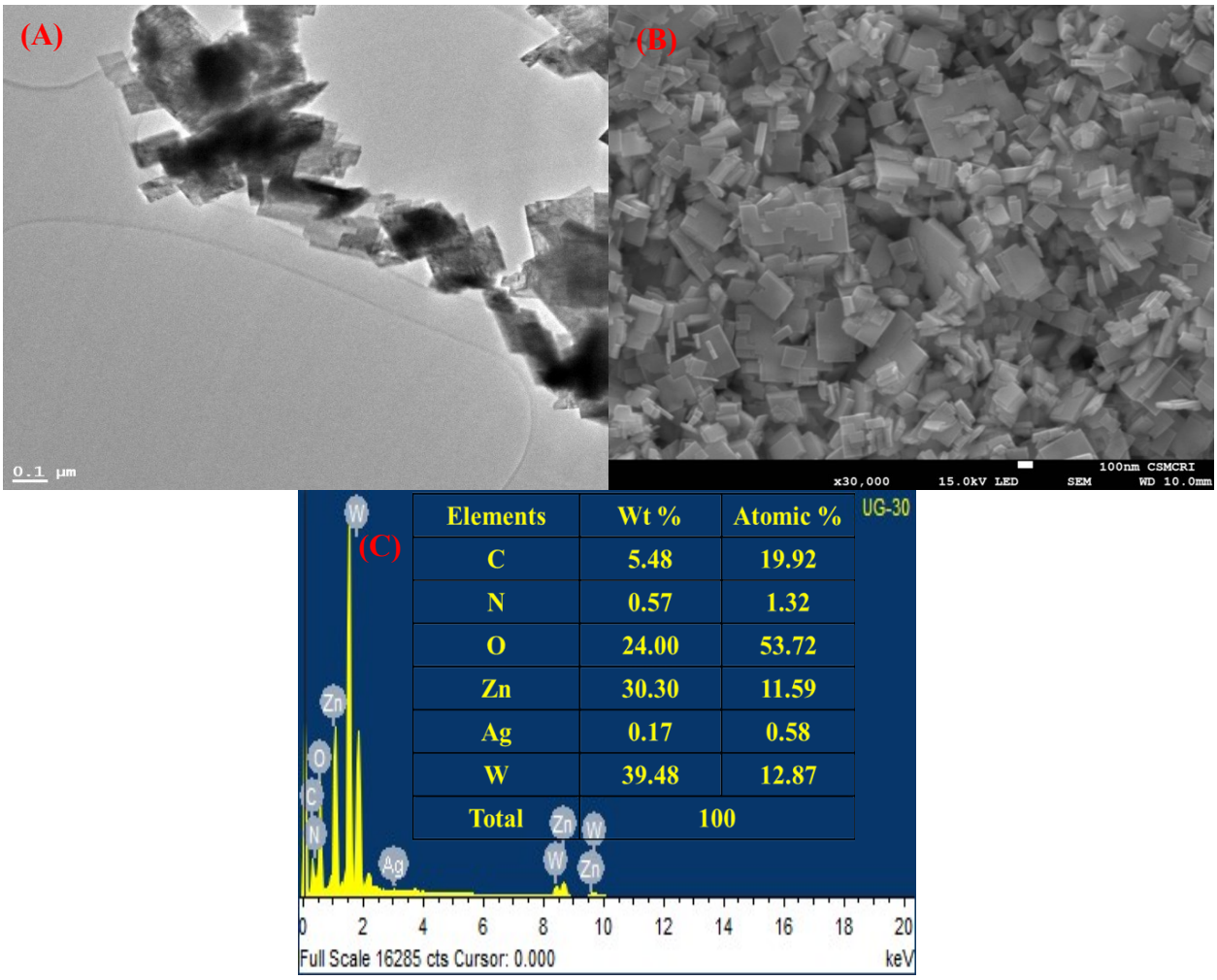

Elements	Wt %	Atomic %
C	5.48	19.92
N	0.57	1.32
O	24.00	53.72
Zn	30.30	11.59
Ag	0.17	0.58
W	39.48	12.87
Total	100	

Figure S17: TEM image (A), FESEM (B), and EDX (C) of g-C_3N_4/Ag/$ZnWO_4$ after multiple cycles of the sensing.

Table S5: Comparison table of Hg^{2+} sensing efficiency for different materials obtained by Fluorescence Spectroscopy

Fluorescence NPs	Method	Detection limit	Linear range	Year	Reference
DNA-AuNP	Fluorescence	25nM	0.05-2.5µM	2008	5
CdS-encapsulated DNA	Fluorescence	4.3nM at 50°C 8.6nM at 30°C	0.04-13 µM	2009	6
Fluorescent Ag clusters	Fluorescence	10nM	10nM-5µM	2011	7
Au@Ag core−shell nanoparticles	Fluorescence	9nM	10-450nM	2011	8
Lysozyme-stabilized Ag nanoclusters	Fluorescence	0.6µM	1-15µM	2012	9
CNP	Fluorescence	2.3nM	5-10nM	2012	10
CDs	Fluorescence	4.2nM	0-3µM	2012	11
Ag NPR	Colorimetric	3.3nM	10-500nM	2013	12
Functionalized Au NPs	Colorimetric	2.9nM	10nM-1.5µM	2014	13
Perylene based Au NPs	Fluorescence	5nM	0-3.5µM	2016	14
Triangular Ag Nanoprism	Colorimetric	30nM (naked eye) 3nM (UV-Vis)	25-800nM	2016	4
NDPP	Fluorescence	11nM	0-4µM	2017	15
AuNPs/CDs	Colorimetric	7.5nM	10-300nM	2018	16
Calixarene-capped Ag NPs	Colorimetric Amperometric	0.5nM	20nM-0.9µM	2019	17
g-C_3N_4/Ag/$ZnWO_4$	**Fluorescence**	**0.23nM**	**0nM-2µM**		**This Work**

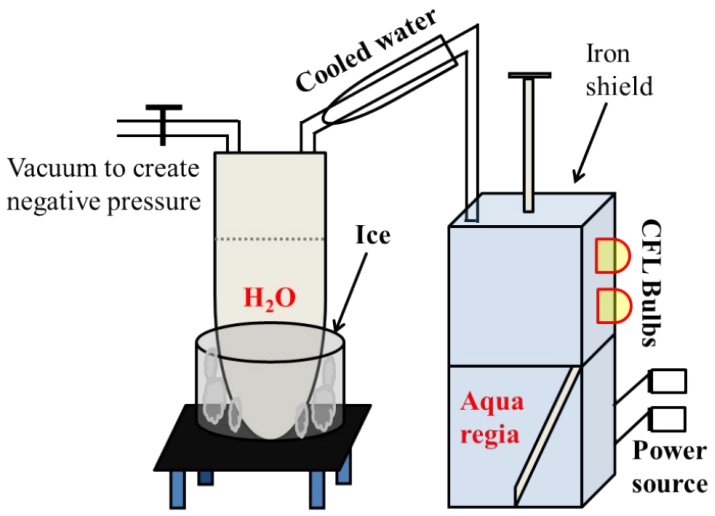

Figure S18: Schematic representation of the extraction of Hg^{2+} from CFL bulbs.

Extraction of mercury from waste CFL bulbs:

Generally, the CFL bulbs contain 4mg of Hg. This mercury was extracted by a chemical method of the efficacy of broken glass, as shown in Figure S18. The waste CFL bulbs were fixed to the closed iron shield container and were crushed by the piston. The broken glass pieces were dropped on to a solution of aqua regia present in a chamber in the vessel and boiled at ~380°C for 30 min. The system was vacuumed to create a negative pressure so that the vapor was then condensed to dissolve in water. The stock solution of mercury was collected and performed PL analysis.

REFERENCES:

1. F. Wang, W. Li, S. Gu, H. Li, X. Liu, M. Wang, *ACS sustainable chemistry & engineering,* 2016, **4**, 6288-6298.
2. B. Ghaemi, E. Shaabani, R. Najafi-Taher, S. J. Nodooshan, A. Sadeghpour, S. Kharrazi, A. Amani, *ACS Applied Materials & Interfaces,* 2018, **10**, 24370-24381.
3. K. Patir, S. K. Gogoi, *ACS Sustainable Chem. Eng.*, 2018, **6**, 1732-1743.
4. N. Chen, Y. Zhang, H. Liu, X. Wu, Y. Li, L. Miao, Z. Shen, A. Wu, *ACS Sens.*, 2016, **1**, 521−527.
5. C.-W. Liu, C.-C. Huang, H.-T. Chang, *Langmuir,* 2008, **24**, 8346-8350.
6. Y. Long, D. Jiang, X. Zhu, J. Wang, F. Zhou, *Anal. Chem.*, 2009, **81**, 2652-2657.
7. C. Guo, J. Irudayaraj, *Anal. Chem.*, 2011, **83**, 2883-2889.
8. S. Guha, S. Roy, A. Banerjee, *Langmuir,* 2011, **27**, 13198-13205.
9. T. Zhou, Y. Huang, W. Li, Z. Cai, F. Luo, C. J. Yang, X. Chen*, Nanoscale*, 2012, **4**, 5312-5315.
10. L. Zhou, Y. Lin, Z. Huang, J. Ren, X. Qu, *Chem. Commun.*, 2012, **48**, 1147-1149.
11. W. Lu, X. Qin, S. Liu, G. Chang, Y. Zhang, Y. Luo, A. M. Asiri, A. O. Al-Youbi, X. Sun, *Anal. Chem.*, 2012, **84**, 5351-5357.
12. L. Chen, X. Fu, W. Lu, L. Chen, *ACS Appl. Mater. Interfaces*, 2013, **5**, 284−290.
13. L. Chen, J. Li, L. Chen, *ACS Appl. Mater. Interfaces*, 2014, **6**, 15897-15904.
14. J. Li, J. Chen, Y. Chen, Y. Li, S.A. Shahzad, Y. Wang, M. Yang, C. Yu, *Analyst*, 2016, **141**, 346–351.
15. K. Nie, B. Dong, H. Shi, Z. Liu, B. Liang, *Anal. Chem*., 2017, **89**, 2928-2936.
16. F. Wang, J. Sun, Y. Lu, X. Zhang, P. Song, Y. Liu, *Analyst*, 2018, **143**, 4741–4746.
17. G. Vyas, S. Bhatt, P. Paul, *ACS Omega,* 2019, **4**, 3860-3870.